KSÜ Mühendislik Bilimleri Dergisi, 27(4), 2024
Araştırma Makalesi

KSU J Eng Sci, 27(4), 2024
Research Article

Kahramanmaras Sutcu Imam University
Journal of Engineering Sciences

Geliş Tarihi : 03.05.2024
Kabul Tarihi : 07.10.2024

Received Date : 03.05.2024
Accepted Date : 07.10.2024

# ENERGY AND ENVIRONMENTAL ANALYSIS OF TRANSCRITICAL $CO_2$ SUPERMARKET REFRIGERATION CYCLES WITH DEDICATED MECHANICAL SUBCOOLER

# ÖZEL MEKANİK AŞIRI SOĞUTUCULU TRANSKRİTİK $CO_2$ SÜPERMARKET SOĞUTMA ÇEVRİMLERİNİN ENERJİ VE ÇEVRESEL ANALİZİ

*Oğuz ÇALIŞKAN*[1,*] (ORCID: 0000-0002-3364-1360)
*H. Kürşad ERSOY*[1] (ORCID: 0000-0001-8588-296X)

[1] Konya Technical University, Department of Mechanical Engineering, Konya, Türkiye

*Sorumlu Yazar / Corresponding Author: Oğuz ÇALIŞKAN, ocaliskan@ktun.edu.tr

**ABSTRACT**

Refrigerants with high environmental impact are being prohibited by legal authorities. The commercial refrigeration sector, a huge contributor to emissions, is transitioning to environmentally friendly $CO_2$ systems. Despite the environmental benefits of $CO_2$, its low critical temperature and high operation pressure can lead to lower performance in warm climates compared to other refrigerants. Therefore, performance improvements are being made for transcritical $CO_2$ refrigeration cycles. This paper presents energy and environmental analysis of transcritical booster (BRC), parallel compression (PRC), and ejector expansion (ERC) supermarket refrigeration cycles with dedicated mechanical subcooler (DMS) as well as transcritical cycles without DMS circuits, and subcritical R404A conventional system. R134a, R1234yf, and R290 were studied as working fluids for DMS circuits. Annual energy consumption and total equivalent warming impact (TEWI) values were compared for İstanbul, Konya, and Samsun in Türkiye, which are in different climate zones, as a case study. The case study constitutes the novelty of this paper. Up to 11% annual energy savings were obtained using $CO_2$ cycles with DMS compared to R404A conventional system. $CO_2$ cycles have up to 58.4% lower total TEWI values than R404A conventional system.

**Keywords:** carbon dioxide, dedicated mechanical subcooler, ejector, environmental impact, supermarket refrigeration

**ÖZET**

Yüksek çevresel etkiye sahip soğutucu akışkanlar resmi otoriteler tarafından yasaklanmaktadır. Emisyonlara büyük katkıda bulunan ticari soğutma sektörü, çevre dostu $CO_2$ sistemlerine geçiş yapmaktadır. Çevresel faydalarına rağmen $CO_2$'nin düşük kritik sıcaklığı ve yüksek çalışma basıncı, sıcak iklimlerde diğer soğutucu akışkanlara kıyasla daha düşük performansa yol açabilir. Bu nedenle transkritik $CO_2$ soğutma çevrimleri için performans iyileştirmeleri yapılmaktadır. Bu makale, özel mekanik aşırı soğutuculu (DMS) çift kademeli (BRC), paralel sıkıştırmalı (PRC) ve ejektör genleşmeli (ERC) transkritik süpermarket soğutma çevrimlerinin yanı sıra DMS'siz çevrimlerin ve kritik nokta altı klasik R404A sistemin enerji ve çevresel analizini sunmaktadır. DMS devreleri için iş akışkanı olarak R134a, R1234yf ve R290 incelenmiştir. Yıllık enerji tüketimi ve toplam eşdeğer ısınma etkisi (TEWI) değerleri, bir uygulama örneği olarak Türkiye'de farklı iklim bölgelerinde yer alan İstanbul, Konya ve Samsun için karşılaştırılmıştır. Uygulama örneği bu çalışmanın özgünlüğünü oluşturmaktadır. R404A klasik sisteme kıyasla DMS'li $CO_2$ çevrimleri kullanılarak yıllık %11'e varan enerji tasarrufu elde edilmiştir. $CO_2$ çevrimleri, R404A klasik sisteme göre %58.4'e kadar daha düşük toplam TEWI değerlerine sahiptir.

**Anahtar Kelimeler:** karbon dioksit, özel mekanik aşırı soğutucu, ejektör, çevresel etki, süpermarket soğutması

ToCite: ÇALIŞKAN, O., & ERSOY, H. K., (2024). ENERGY AND ENVIRONMENTAL ANALYSIS OF TRANSCRITICAL CO2 SUPERMARKET REFRIGERATION CYCLES WITH DEDICATED MECHANICAL SUBCOOLER. *Kahramanmaraş Sütçü İmam Üniversitesi Mühendislik Bilimleri Dergisi*, 27(4), 1582-1601.

## INTRODUCTION

Commercial refrigerators are systems that preserve fresh (chilled) and frozen food at desired temperatures in supermarkets, grocery stores, and convenience stores. Commercial refrigeration systems are the biggest energy users within supermarkets, accounting for about 40 to 60% of electricity consumption (Klemick, Kopits, and Wolverton, 2015). On a global basis, commercial refrigeration is the refrigeration subsector with the largest refrigerant emissions calculated as $CO_2$ equivalents, which represents 40% of the total annual refrigerant emissions (Devotta and Sicars, 2005).

The properties of common refrigerants used in commercial refrigeration systems are presented in Table 1 (Bell, Wronski, Quoilin, and Lemort, 2014; Smith et al., 2021). The global warming potential (GWP) values of the refrigerants are defined by the Intergovernmental Panel on Climate Change (IPCC) Assessment Report (AR), which is updated periodically. According to the latest IPCC AR6, GWP values of R1234yf and R290 (propane) are below 1. R404A, R134a, and R744 ($CO_2$) are safe refrigerants while R1234yf is mildly flammable, and R290 is highly flammable.

**Table 1.** Properties of Common Refrigerants Used in Commercial Refrigerators (Bell et al., 2014; Smith et al., 2021)

| Property | R404A | R134a | R1234yf | R744 ($CO_2$) | R290 (Propane) |
|---|---|---|---|---|---|
| 100-year GWP | 4728 | 1530 | 0.501 | 1 | 0.02 |
| Critical temperature [°C] | 72.12 | 101.06 | 94.7 | 90.98 | 96.74 |
| Critical pressure [bar] | 37.35 | 40.59 | 33.82 | 73.77 | 42.51 |
| Normal boiling temperature [°C] | -45.47 | -26.07 | -29.49 | -78.46 | -42.12 |
| Saturation pressure at 0 °C [bar] | 6 | 2.93 | 3.16 | 34.85 | 4.75 |
| Vaporization enthalpy at 0 °C [kJ/kg] | 165.82 | 198.6 | 163.29 | 230.89 | 374.87 |
| Vapor density at 0 °C [kg/m$^3$] | 30.46 | 14.43 | 17.65 | 97.65 | 10.35 |
| Safety class | A1 | A1 | A2L | A1 | A3 |

The use of hydrofluorocarbons (HFCs) with a GWP above 2500 has been prohibited in all new commercial refrigeration equipment as of January 1st, 2020, and the use of HFCs with a GWP above 150 excluding primary refrigerants of cascade systems with GWP values lower than 1500 has been prohibited in new commercial refrigeration systems with a rated capacity of 40 kW or more placed in the EU market as of January 1st, 2022, by the F-Gas regulation (Schulz and Kourkoulas, 2014). The use of R404A with a GWP value of 4728 according to IPCC AR6 (Smith et al., 2021), which is a common refrigerant in commercial refrigerators, is not possible in the newly installed systems in the European market. The GWP value of R134a is defined as 1430 by the F-Gas regulation (Schulz and Kourkoulas, 2014), in contrast to 1530 declared by the IPCC AR6 (Smith et al., 2021), which makes it possible to use in cascade systems.

There is a significant trend towards the use of transcritical $CO_2$ refrigeration systems in the food retail sector because $CO_2$ is cheap, non-toxic, and non-flammable. As of December 2023, approximately 68500 food retail stores in Europe, 2930 in North America, and 8385 in Japan use transcritical $CO_2$ systems. The market penetration of transcritical $CO_2$ systems is 22.9% in Europe, 1.27% in North America, and 10.9% in Japan, which is increasing every year (Hayes, Haroldsen, and Thapa, 2023). ALDI US, the leading grocery user of transcritical $CO_2$ systems in the US, has announced that all of its stores will use natural refrigerants by 2035 (Hines, 2024). Germany-based food wholesaler METRO installed Serbia's first transcritical $CO_2$ system in Belgrade in November 2023 (Hayes, 2024). Japanese convenience store chain Lawson operates over 34% of its stores with outdoor $CO_2$ condensing units (Haroldsen, 2023). France-based supermarket chain Carrefour has two stores in İstanbul with $CO_2$ systems installed. One of these systems, located in Bahçelievler, is an R404A/$CO_2$ cascade system, whereas the other one, located in Kurtköy, is a transcritical booster system equipped with an adiabatic gas cooler (Chakroun, 2016; Papazahariou, 2010). Olaf Schulze, Director of Energy Management and Real Estate Sustainability at METRO Properties, stated that the company's plans to install transcritical $CO_2$ equipment in Türkiye have been delayed due to a lack of service technicians, hoping the installation can take place next year (Hayes, 2023).

Despite the benefits of $CO_2$ as a refrigerant, it has a lower critical temperature and higher operation pressure than HFCs, which can lead to lower performance at high ambient temperatures. Various improvements are being made to enhance the performance of the $CO_2$ systems at high ambient temperatures including parallel compression, ejector expansion, and dedicated mechanical subcooling.

A theoretical comparison of different transcritical $CO_2$ supermarket refrigeration cycle configurations was performed by Isik and Bilir Sag (2023) for 12 provinces in Türkiye, suggesting the cycle with parallel compression and flooded evaporators because it consumes less energy, has lower emissions, and has a reasonable payback period for each investigated province. Atmaca et al. (2018) parametrically investigated a one-stage transcritical refrigeration cycle with ejector expansion that uses $CO_2$, ethane, and fluoromethane as working fluids. The authors indicated that the performance improvement potential for $CO_2$ and methane is about 20%, whereas it is about 14% for fluoromethane at various evaporator temperatures. Sengupta and Dasgupta (2023) presented a novel dual ejector-based transcritical $CO_2$ supermarket refrigeration cycle and compared it with R404A conventional cycle, obtaining 11.35% annual energy savings and 31% TEWI reduction for Seville. Dai et al. (2024) modeled different transcritical $CO_2$ supermarket refrigeration cycle configurations with parallel compressor and dedicated mechanical subcooler, obtaining 9.85% lower annual energy consumption and up to 6.87% lower carbon emission with the use of triple-stage dedicated mechanical subcooler compared to the base cycle. Liu et al. (2021) proposed a transcritical $CO_2$ supermarket refrigeration cycle using multi-ejector and dedicated mechanical subcooler. The authors indicated that the proposed cycle has a 61.76% higher COP than the basic booster cycle at the ambient temperature of 40 °C.

This paper presents energy and environmental analysis of transcritical booster (BRC), parallel compression (PRC), and ejector expansion (ERC) supermarket refrigeration cycles with dedicated mechanical subcooler (DMS) as well as transcritical cycles without DMS circuits, and R404A conventional system. R134a, R1234yf, and R290 were studied as working fluids for DMS circuits. Although R404A is prohibited for newly installed systems, it is widely used in actual supermarket refrigeration systems which are allowed to operate for the next years (Tsimpoukis et al., 2021). The aim of the comparison with R404A is to show the energy and environmental superiority of $CO_2$ cycles against a widely used refrigerant. As a case study, annual energy consumption and total equivalent warming impact (TEWI) values were compared for three provinces in Türkiye, which are in different climate zones. Annual energy and TEWI analysis of transcritical cycles with DMS circuits for different climate regions in Türkiye constitute the novelty of this paper.

## CYCLE MODELING

Transcritical booster supermarket refrigeration cycle (BRC) with dedicated mechanical subcooler (DMS) is presented in Figure 1. The cycle consists of medium-temperature (chiller) and low-temperature (freezer) evaporators. The high-pressure refrigerant at the gas cooler outlet is subcooled via the DMS evaporator to lower its enthalpy. The heat absorbed by the DMS evaporator is rejected through the condenser of the DMS circuit. Subcooled refrigerant is expanded to an intermediate pressure level through the high-pressure expansion valve (HXPV). In the flash tank, liquid and vapor streams are separated. Vapor is expanded to the chiller pressure by the flash-gas-bypass (FGB) valve while liquid is sent to the medium-pressure expansion valve (MPXV) and low-pressure expansion valve (LPXV). Refrigerant at the freezer outlet is compressed to the chiller pressure through the low-pressure compressor (LPC). Then, three streams are mixed before the high-pressure compressor (HPC) and compressed to the gas cooler pressure. Heat rejection with no phase change occurs in the gas cooler under transcritical operation.

Figure 2 shows parallel compression supermarket refrigeration cycle (PRC) with dedicated mechanical subcooler (DMS). As opposed to BRC, the vapor stream at the flash tank is compressed through a separate parallel compressor (PC) to reduce the compressor work instead of expanding to the chiller pressure. It consists of an FGB valve in case of insufficient mass flow in the PC to bypass through HPC.

HPXV is replaced by the ejector in the ejector expansion supermarket refrigeration cycle (ERC) with dedicated mechanical subcooler (DMS) as shown in Figure 3. The ejector acts as a pressure recovery component to increase the suction pressure of the HPC.

The cycles were modeled in MATLAB environment using the CoolProp library for the thermophysical properties of the refrigerants (Bell et al., 2014; The MathWorks Inc., 2022). The following assumptions were made for the calculations:

- All cycles operate at a steady state.

- Chiller evaporator temperature ($T_{MT}$) and design capacity ($\dot{Q}_{MT}$) values were taken as -8 °C and 80 kW, respectively (Tsimpoukis et al., 2021).
- Freezer evaporator temperature ($T_{LT}$) and design capacity ($\dot{Q}_{LT}$) values were taken as -32 °C and 25 kW, respectively (Tsimpoukis et al., 2021).
- 10 K of internal (useful) superheat was considered for each $CO_2$ evaporator (Tsimpoukis et al., 2021).
- 5 K of external superheat was considered for DMS heat exchanger evaporator (Catalán-Gil, Llopis, Sánchez, Nebot-Andrés, and Cabello, 2019).
- Condenser/gas cooler conditions for the $CO_2$ cycles depending on the ambient temperature ($T_{amb}$) were taken as shown in Table 2 (Tsimpoukis et al., 2021).
- Condenser conditions for R404A conventional system and DMS cycles depending on the ambient temperature ($T_{amb}$) were taken as shown in Table 3 (Tsimpoukis et al., 2021).
- Global efficiency correlations shown in Table 4 were considered for compressors depending on pressure ratio ($R_p$) (de Paula, Duarte, Rocha, de Oliveira, and Maia, 2020; de Paula, Duarte, Rocha, de Oliveira, Mendes, et al., 2020; Tsimpoukis et al., 2021).
- 95% constant mechanical efficiency was considered for each compressor (Mitsopoulos et al., 2019).
- DMS heat exchanger effectiveness was taken as 60% for each cycle (Catalán-Gil et al., 2019).
- Ejector component efficiency values were taken as $\eta_{mn} = 90\%$ for motive nozzle, $\eta_{sn} = 90\%$ for suction nozzle, and $\eta_{dif} = 80\%$ for diffuser (Li and Groll, 2005).
- Pressure drops in the piping and heat exchangers were not considered.
- Heat losses in the piping were not considered.
- Expansion processes in the expansion valves were considered as isentalphic.
- Electricity consumption of the evaporator and condenser/gas cooler fans was taken as 3% of the heat transfer rate of the corresponding heat exchanger (Karampour and Sawalha, 2018).
- R404A system was considered as subcritical separate cycles for the chiller and freezer (Mitsopoulos et al., 2019).

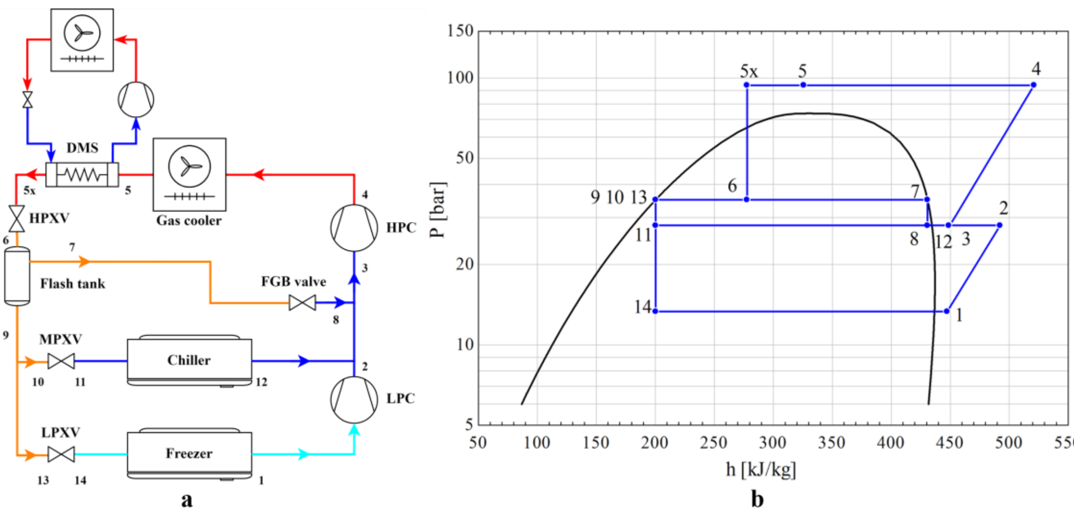


**Figure 1.** Transcritical Booster Supermarket Refrigeration Cycle (BRC) with Dedicated Mechanical Subcooler (DMS) **a.** Plant Layout, **b.** Pressure-Enthalpy Diagram (Klein, 2020)

Evaporator loads vary between a minimum value and design value depending on the ambient temperature. Evaporator loads are at minimum value when the ambient temperature is below 5 °C. Between the ambient temperatures of 5 and 30 °C, evaporator loads were calculated using Eq. (1). Minimum fraction ($mf$) was taken as 0.66 for the chiller, and 0.80 for the freezer. When the ambient temperature is above 30 °C, evaporator loads are at design value. This is because when the ambient temperature deviates from the design point, the indoor air temperature and relative humidity will change and this will cause refrigeration loads to deviate from the design loads defined by the store refrigeration schedule (Zhang, 2006).

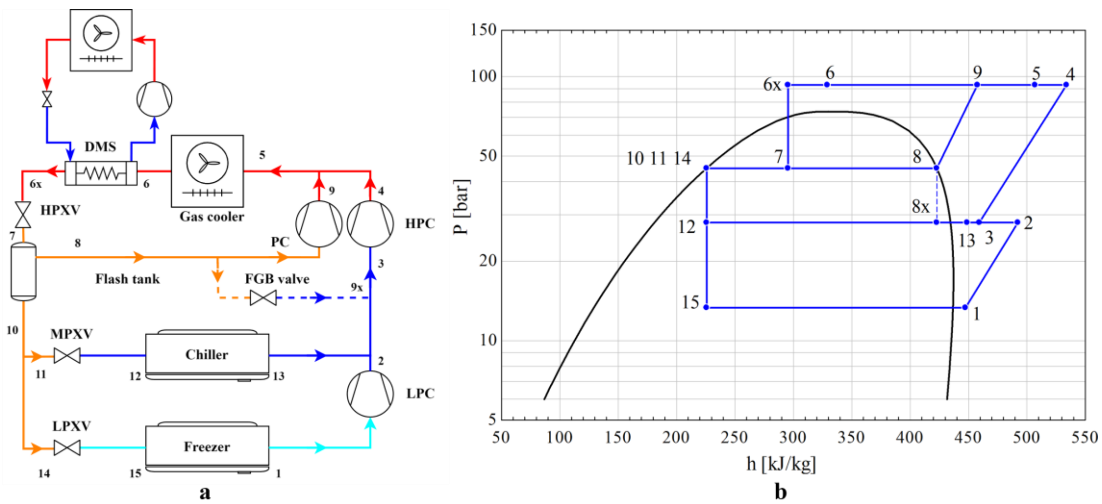


**Figure 2.** Parallel Compression Transcritical Supermarket Refrigeration Cycle (PRC) with Dedicated Mechanical Subcooler (DMS) **a.** Plant Layout, **b.** Pressure-Enthalpy Diagram (Klein, 2020)

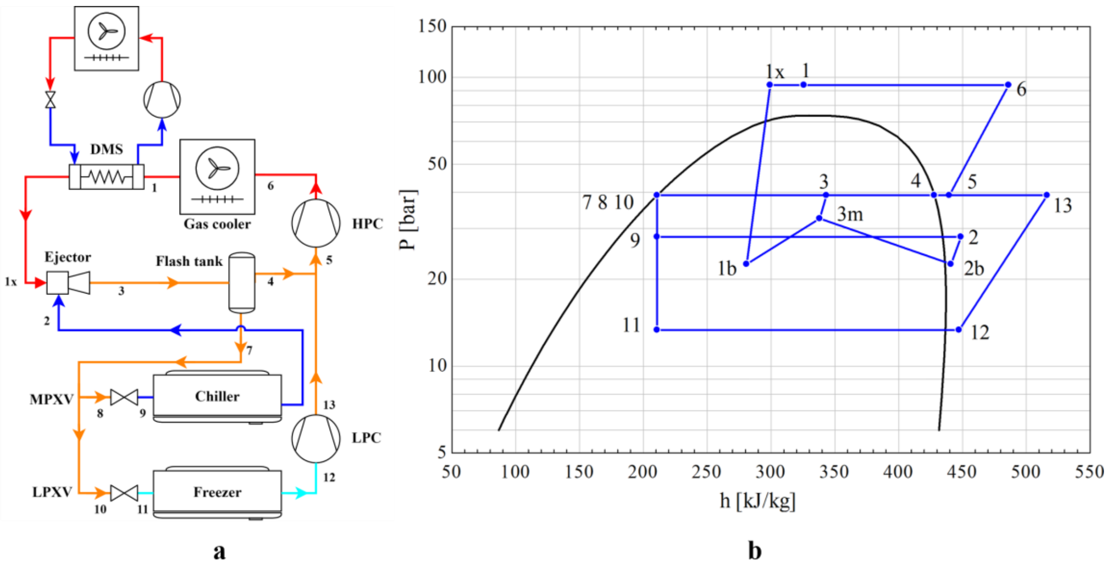


**Figure 3.** Ejector Expansion Transcritical Supermarket Refrigeration Cycle (ERC) with Dedicated Mechanical Subcooler (DMS) **a.** Plant Layout, **b.** Pressure-Enthalpy Diagram (Klein, 2020)

**Table 2.** Condenser/Gas Cooler Conditions for $CO_2$ Cycles (Tsimpoukis et al., 2021)

| $T_{amb}$ [°C] | $T_{cond/GC,out}$ [°C] | $P_{cond/GC}$ [bar] |
|---|---|---|
| $T_{amb} \leq 5$ | 11 | Saturated pressure at 13 °C |
| $5 < T_{amb} \leq 14$ | $T_{amb} + 6$ | Saturated pressure at $T_{amb} + 8$ °C |
| $14 < T_{amb} \leq 27$ | $0.7692T_{amb} + 9.23$ | $1.397T_{GC,out} + 32.09$ |
| $T_{amb} > 27$ | $T_{amb} + 3$ | Optimized (transcritical) |

**Table 3.** Condenser Conditions for R404A Conventional System and DMS Cycles (Tsimpoukis et al., 2021)

| $T_{amb}$ [°C] | $T_{cond,out}$ [°C] | $P_{cond}$ [bar] |
|---|---|---|
| $T_{amb} \leq 19$ | 25 | Saturated pressure at 27 °C |
| $T_{amb} > 19$ | $T_{amb} + 6$ | Saturated pressure at $T_{amb} + 8$ °C |

$$\dot{Q}_{ev} = \left[1 - (1 - mf)\left(\frac{30 - T_{amb}}{30 - 5}\right)\right]\dot{Q}_{ev,design} \quad \text{if } 5 \leq T_{amb} \leq 30 \text{ °C} \tag{1}$$

Evaporation temperature ($T_{ev,DMS}$) and capacity ($\dot{Q}_{DMS}$) of the DMS circuit was determined using Eqs. (2-3) (Catalán-Gil et al., 2019).

$$T_{ev,DMS} = T_{DMS,in,CO_2} - \frac{\left(T_{DMS,in,CO_2} - T_{DMS,out,CO_2}\right)}{\varepsilon_{DMS}} \tag{2}$$

$$\dot{Q}_{DMS} = \dot{m}_{GC}(h_{DMS,in,CO_2} - h_{DMS,out,CO_2}) \tag{3}$$

Where $T_{DMS,in,CO_2}$ is gas cooler outlet temperature of $CO_2$, $T_{DMS,out,CO_2}$ is DMS outlet temperature of $CO_2$, and $\varepsilon_{DMS}$ is DMS heat exchanger effectiveness, $\dot{m}_{GC}$ is the gas cooler mass flow rate, $h_{DMS,in,CO_2}$ is enthalpy of $CO_2$ at DMS inlet, $h_{DMS,out,CO_2}$ is enthalpy of $CO_2$ at DMS outlet.

**Table 4.** Global Compressor Efficiency Correlations (de Paula, Duarte, Rocha, de Oliveira, and Maia, 2020; de Paula, Duarte, Rocha, de Oliveira, Mendes, et al., 2020; Tsimpoukis et al., 2021)

| System | Global Efficiency of the Compressors |
|---|---|
| $CO_2$ | $\eta_{glob,LPC} = -0.0257R_p^2 + 0.1085R_p + 0.5890$ |
| | $\eta_{glob,HPC} = -0.0265R_p^2 + 0.1572R_p + 0.5221$ |
| | $\eta_{glob,PC} = -0.0457R_p^2 + 0.2698R_p + 0.3582$ |
| R134a DMS | $\eta_{glob,DMS} = -0.0058R_p^2 + 0.0766R_p + 0.2819$ |
| R1234yf DMS | $\eta_{glob,DMS} = 0.0018R_p^3 - 0.0342R_p^2 + 0.2012R_p + 0.0499$ |
| R290 DMS | $\eta_{glob,DMS} = -0.0131R_p^2 + 0.1256R_p + 0.2392$ |
| R404A | $\eta_{glob,LPC} = -0.0014R_p^2 + 0.0044R_p + 0.6080$ |
| | $\eta_{glob,HPC} = -0.0216R_p^2 + 0.1423R_p + 0.4664$ |

Energy equations for the components of the main cycles are given in Table 5.

**Table 5.** Energy Equations for the Components of the Main Cycles

| Component | BRC | PRC | ERC |
|---|---|---|---|
| Low-pressure compressor (LPC) | $h_{2,is} = f(P_2, s_1)$ | $h_{2,is} = f(P_2, s_1)$ | $h_{13,is} = f(P_{13}, s_{12})$ |
| | $h_2 = h_1 + \frac{h_{2,is} - h_1}{\eta_{LPC,is}}$ | $h_2 = h_1 + \frac{h_{2,is} - h_1}{\eta_{LPC,is}}$ | $h_{13} = h_{12} + \frac{h_{13,is} - h_{12}}{\eta_{LPC,is}}$ |
| | $\dot{W}_{LPC} = \dot{m}_{LT}\frac{h_{2,is} - h_1}{\eta_{LPC,glob}}$ | $\dot{W}_{LPC} = \dot{m}_{LT}\frac{h_{2,is} - h_1}{\eta_{LPC,glob}}$ | $\dot{W}_{LPC} = \dot{m}_{LT}\frac{h_{13,is} - h_{12}}{\eta_{LPC,glob}}$ |
| High-pressure compressor (HPC) | $\dot{m}_{HPC} = \dot{m}_{LT} + \dot{m}_{MT} + \dot{m}_{FGB}$ | $\dot{m}_{HPC} = \dot{m}_{LT} + \dot{m}_{MT}$ | $\dot{m}_{HPC} = \dot{m}_{LT} + \dot{m}_{FGB}$ |
| | $h_3 = \frac{\dot{m}_{LT}h_2 + \dot{m}_{MT}h_{12} + \dot{m}_{FGB}h_8}{\dot{m}_{HPC}}$ | $h_3 = \frac{\dot{m}_{LT}h_2 + \dot{m}_{MT}h_{13}}{\dot{m}_{HPC}}$ | $h_5 = \frac{\dot{m}_{LT}h_{13} + \dot{m}_{FGB}h_4}{\dot{m}_{HPC}}$ |
| | $s_3 = f(P_{MT}, h_3)$ | $s_3 = f(P_{MT}, h_3)$ | $s_5 = f(P_3, h_5)$ |
| | $h_{4,is} = f(P_4, s_3)$ | $h_{4,is} = f(P_4, s_3)$ | $h_{6,is} = f(P_6, s_5)$ |
| | $h_4 = h_3 + \frac{h_{4,is} - h_3}{\eta_{HPC,is}}$ | $h_4 = h_3 + \frac{h_{4,is} - h_3}{\eta_{HPC,is}}$ | $h_6 = h_5 + \frac{h_{6,is} - h_5}{\eta_{HPC,is}}$ |
| | $\dot{W}_{HPC} = \dot{m}_{HPC}\frac{h_{4,is} - h_3}{\eta_{HPC,glob}}$ | $\dot{W}_{HPC} = \dot{m}_{HPC}\frac{h_{4,is} - h_3}{\eta_{HPC,glob}}$ | $\dot{W}_{HPC} = \dot{m}_{HPC}\frac{h_{6,is} - h_5}{\eta_{HPC,glob}}$ |
| Parallel compressor (PC) | | $h_{9,is} = f(P_9, s_8)$ | |
| | | $h_9 = h_8 + \frac{h_{9,is} - h_8}{\eta_{PC,is}}$ | |
| | | $\dot{W}_{PC} = \dot{m}_{FGB}\frac{h_{9,is} - h_8}{\eta_{PC,glob}}$ | |
| Freezer | $h_1 = f\left(P_{LT}, T_{LT} + \Delta T_{SH,LT}\right)$ | $h_1 = f\left(P_{LT}, T_{LT} + \Delta T_{SH,LT}\right)$ | $h_{12} = f\left(P_{LT}, T_{LT} + \Delta T_{SH,LT}\right)$ |
| | $s_1 = f\left(P_{LT}, T_{LT} + \Delta T_{SH,LT}\right)$ | $s_1 = f\left(P_{LT}, T_{LT} + \Delta T_{SH,LT}\right)$ | $s_{12} = f\left(P_{LT}, T_{LT} + \Delta T_{SH,LT}\right)$ |

| | | | |
|---|---|---|---|
| Chiller | $\dot{m}_{LT} = \frac{\dot{Q}_{LT}}{h_1 - h_{14}}$<br>$h_{12} = f(P_{MT}, T_{MT} + \Delta T_{SH,MT})$<br>$\dot{m}_{MT} = \frac{\dot{Q}_{MT}}{h_{12} - h_{11}}$<br>$h_{5x} = f(P_{GC}, T_{5x})$ | $\dot{m}_{LT} = \frac{\dot{Q}_{LT}}{h_1 - h_{15}}$<br>$h_{13} = f(P_{MT}, T_{MT} + \Delta T_{SH,MT})$<br>$\dot{m}_{MT} = \frac{\dot{Q}_{MT}}{h_{13} - h_{12}}$<br>$h_{6x} = f(P_{GC}, T_{6x})$ | $\dot{m}_{LT} = \frac{\dot{Q}_{LT}}{h_{12} - h_{11}}$<br>$h_2 = f(P_{MT}, T_{MT} + \Delta T_{SH,MT})$<br>$\dot{m}_{MT} = \frac{\dot{Q}_{MT}}{h_2 - h_9}$ |
| Expansion valves | $h_{5x} = h_6$ | $h_{6x} = h_7$ | $h_7 = h_8 = h_9 = h_{10} = h_{11}$ |
| Flash-gas-bypass (FGB) valve | $h_9 = h_{10} = h_{11} = h_{13} = h_{14}$<br>$h_7 = h_8$ | $h_{10} = h_{11} = h_{12} = h_{14} = h_{15}$ | |
| Ejector | | | $h_{1x} = f(P_{GC}, T_{1x})$<br>$\dot{m}_3 = \dot{m}_{MT}\left(1 + \frac{1}{\omega}\right)$<br>$h_3 = f(P_3, x_3)$<br>$\dot{m}_1 h_{1x} + \dot{m}_2 h_2 = \dot{m}_3 h_3$ |
| Flash tank | $h_7 = f(P_{FGB}, x = 1)$<br>$h_9 = f(P_{FGB}, x = 0)$<br>$\dot{m}_{FGB} = (\dot{m}_{LT} + \dot{m}_{MT})\left(\frac{h_6 - h_9}{h_7 - h_6}\right)$ | $h_8 = f(P_{FGB}, x = 1)$<br>$s_8 = f(P_{FGB}, x = 1)$<br>$h_{10} = f(P_{FGB}, x = 0)$<br>$\dot{m}_{FGB} = (\dot{m}_{LT} + \dot{m}_{MT})\left(\frac{h_7 - h_{10}}{h_8 - h_7}\right)$<br>$\dot{m}_{GC} = \dot{m}_{HPC} + \dot{m}_{FGB}$ | $h_4 = f(P_3, x = 1)$<br>$h_7 = f(P_3, x = 0)$<br>$\dot{m}_{FGB} = \dot{m}_3 - (\dot{m}_{LT} + \dot{m}_{MT})$ |
| Gas cooler | $h_5 = f(P_{GC}, T_{GC,out})$<br>$\dot{Q}_{GC} = \dot{m}_{HPC}(h_4 - h_5)$ | $h_5 = \frac{\dot{m}_{HPC} h_4 + \dot{m}_{FGB} h_9}{\dot{m}_{GC}}$<br>$\dot{Q}_{GC} = \dot{m}_{GC}(h_5 - h_6)$ | $h_1 = f(P_{GC}, T_{GC,out})$<br>$\dot{Q}_{GC} = \dot{m}_{HPC}(h_6 - h_1)$ |

Table 6 presents energy equations for the components of the DMS cycles.

**Table 6.** Energy Equations for the Components of the Dedicated Mechanical Subcooler (DMS) Cycles

| Component | Energy Equation |
|---|---|
| Compressor | $h_{comp,DMS,out,is} = f(P_{cond,DMS}, s_{ev,DMS,out})$<br>$h_{comp,DMS,out} = h_{ev,DMS,out} + \frac{h_{comp,DMS,out,is} - h_{ev,DMS,out}}{\eta_{comp,DMS,is}}$<br>$\dot{W}_{comp,DMS} = \dot{m}_{DMS}\frac{h_{comp,DMS,out,is} - h_{ev,DMS,out}}{\eta_{comp,DMS,glob}}$ |
| Expansion valve | $h_{cond,DMS,out} = h_{ev,DMS,in}$ |
| Evaporator | $\dot{Q}_{DMS} = \dot{m}_{GC}(h_{DMS,in,CO_2} - h_{DMS,out,CO_2})$<br>$P_{ev,DMS} = f(T_{ev,DMS}, x = 1)$<br>$h_{ev,DMS,out} = f(T_{ev,DMS}, x = 1)$<br>$s_{ev,DMS,out} = f(T_{ev,DMS}, x = 1)$<br>$\dot{m}_{DMS} = \frac{\dot{Q}_{DMS}}{h_{ev,DMS,out} - h_{ev,DMS,in}}$ |
| Condenser | $P_{cond,DMS} = f(T_{cond,DMS}, x = 0)$<br>$h_{cond,DMS,out} = f(P_{cond,DMS}, T_{cond,DMS} - \Delta T_{SC,cond,DMS})$<br>$\dot{Q}_{cond,DMS} = \dot{m}_{DMS}(h_{comp,DMS,out} - h_{cond,DMS,out})$ |

Coefficient of performance (COP) is defined as the ratio of total evaporator capacity to total power consumption of the compressors and fans as shown in Eq. (4).

$$COP = \frac{\dot{Q}_{MT} + \dot{Q}_{LT}}{\sum \dot{W}_{comp} + \sum \dot{W}_{fan}} \tag{4}$$

The ejector consists of a motive nozzle, suction nozzle, mixing chamber, and diffuser. Constant-area flow model was used in the ejector calculations (Caliskan, Bilir Sag, and Ersoy, 2024). The reason why the constant-area flow model is preferred over the constant-pressure flow model is that theoretical results obtained by using the constant-area flow model agree with experimental results as opposed to the constant-pressure flow model (Keenan, Neumann, and Lustwerk, 1950). Additionally, for the same operating temperatures, the calculated COP of the constant-area ejector flow model system is greater than that of the constant pressure ejector flow model system (Yapici and Ersoy, 2005). Entrainment ratio ($\omega$) is the ratio of the suction flow to the motive flow as shown in Eq. (5). Entrainment ratio ($\omega$) and mixing chamber pressure ($P_{3m}$) are optimized to satisfy mass, heat, and momentum balance in the ejector. The solution algorithm for ERC is presented in Figure 4.

$$\omega = \frac{\dot{m}_{sn}}{\dot{m}_{mn}} = \frac{\dot{m}_{MT}}{\dot{m}_{HPC}} \tag{5}$$

Where $\dot{m}_{MT}$ is chiller mass flow rate, $\dot{m}_{HPC}$ is HPC mass flow rate.

The BRC model was validated by an experimental study performed by Tsamos et al. (2017) under the same conditions as stated by the authors. The mean deviation of COP values was calculated as 2.5%. The ejector model was validated by Danfoss Coolselector2 software (Danfoss, 2023), which contains the performance data of commercially available ejectors in the market manufactured by Danfoss. The performance data are based on experimental results (Contiero, Pardiñas, and Hafner, 2021). The mean deviation of entrainment ratio values was calculated as 3.3%.

Bin-hour method was used for annual energy consumption calculations of the cycles. Bin data is defined as the number of hours that the ambient temperature was in each of a set of equally sized intervals of ambient temperature as shown in Eq. (6). In this method, energy consumption calculations are performed at each ambient temperature and these are multiplied by the number of occurrence hours at each ambient temperature (Said, Habib, and Iqbal, 2003).

$$E_{tot} = \sum \left(\dot{W}_{tot} N_{bin}\right)_{@T_{amb}} \tag{6}$$

Total Equivalent Warming Impact (TEWI) method based on the EN378 standard was used for environmental impact calculations of the cycles (Zottl, Lindahl, Nordman, Rivière, and Miara, 2011). Direct TEWI is caused by refrigerant leakage from the system during its lifetime and disposal of the refrigerant at the end of life, while indirect TEWI is caused by electricity generation to operate the system as shown in Eqs. (7-9). Refrigerant charge ($m_{ref}$) was taken as 3 kg/kW for $CO_2$ cycles, 2 kg/kW for DMS and R404A chiller cycles, and 4 kg/kW for R404A freezer cycle (Karampour and Sawalha, 2018). Annual refrigerant leakage ($L$), operation lifetime ($n$), refrigerant recycling factor ($\alpha$), and electricity generation emissions ($K$) were taken as 10% of the refrigerant charge, 15 years, 95%, and 0.44 kg $CO_{2e}$/kWh, respectively (ETKB, 2022; Karampour and Sawalha, 2018).

$$TEWI_{Direct} = GWP \times L \times n + GWP \times m_{ref} \times (1 - \alpha) \tag{7}$$

$$TEWI_{Indirect} = E \times n \times K \tag{8}$$

$$TEWI_{total} = TEWI_{Direct} + TEWI_{Indirect} \tag{9}$$

## RESULTS AND DISCUSSION

The effect of the subcooling degree ($\Delta T_{SC}$) to the performance of the cycles was investigated in Figure 5 for BRC, Figure 6 for PRC, and Figure 7 for ERC under the same operation conditions. With the increase in the subcooling degree, the vapor quality in the flash tank decreases, which leads to lower mass flow rate and lower power consumption in the compressors. However, the mass flow rate in DMS circuit increases due to increased capacity.

The pressure difference in the DMS compressor also increases due to decreased evaporator temperature. Therefore, the power consumption of DMS circuit increases. It can be seen that there is an optimum point of subcooling degree to maximize COP for each cycle. DMS power consumption increases more rapidly than the reduction in power consumption of $CO_2$ cycle above the optimum point, which reduces the total COP. The performance of R134a and R290 DMS circuits are identical. R290 circuit has the lowest mass flow rate due to its highest vaporization enthalpy among investigated refrigerants.

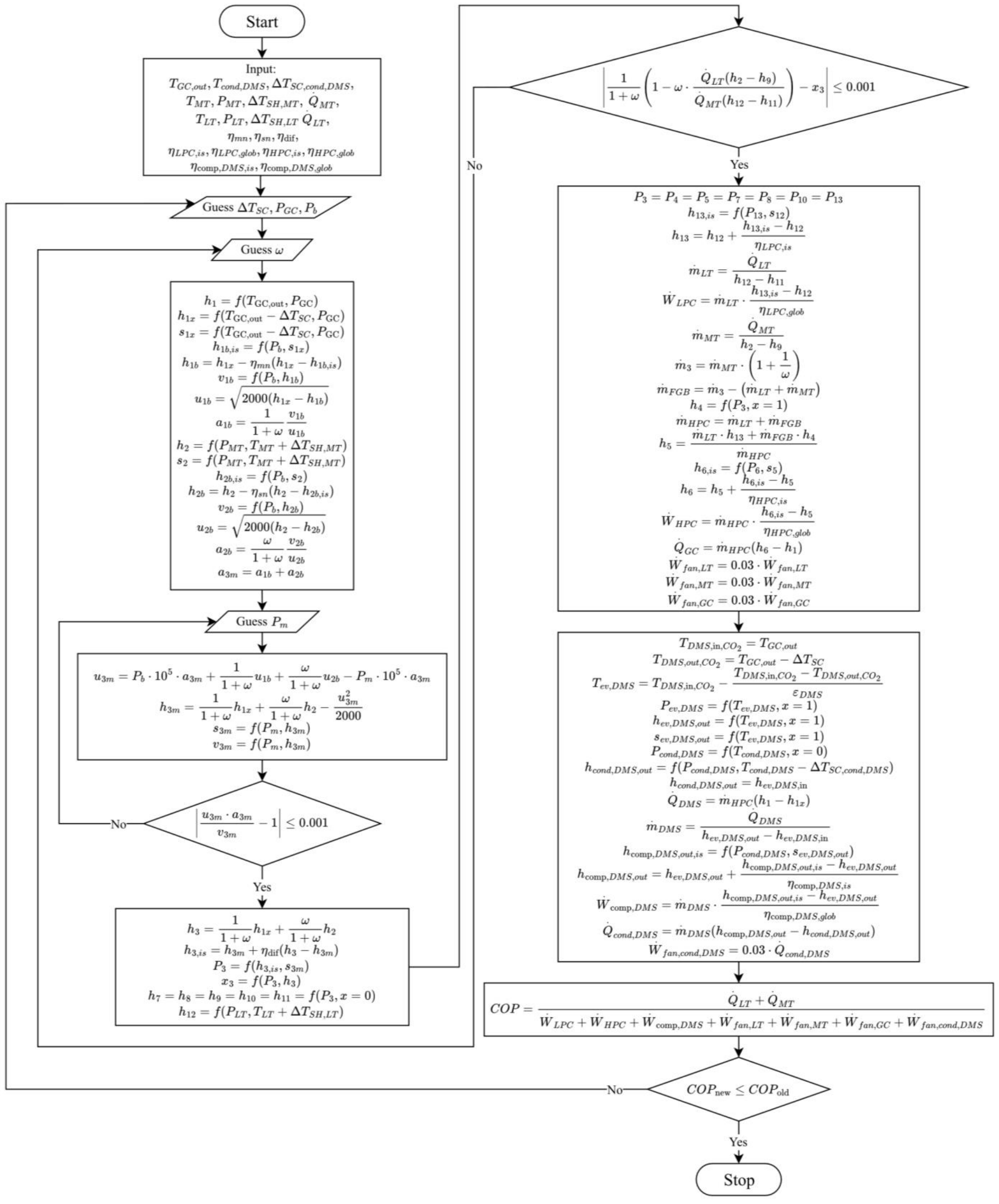


**Figure 4.** Solution Algorithm for Ejector Refrigeration Cycle (ERC) with Dedicated Mechanical Subcooler (DMS)

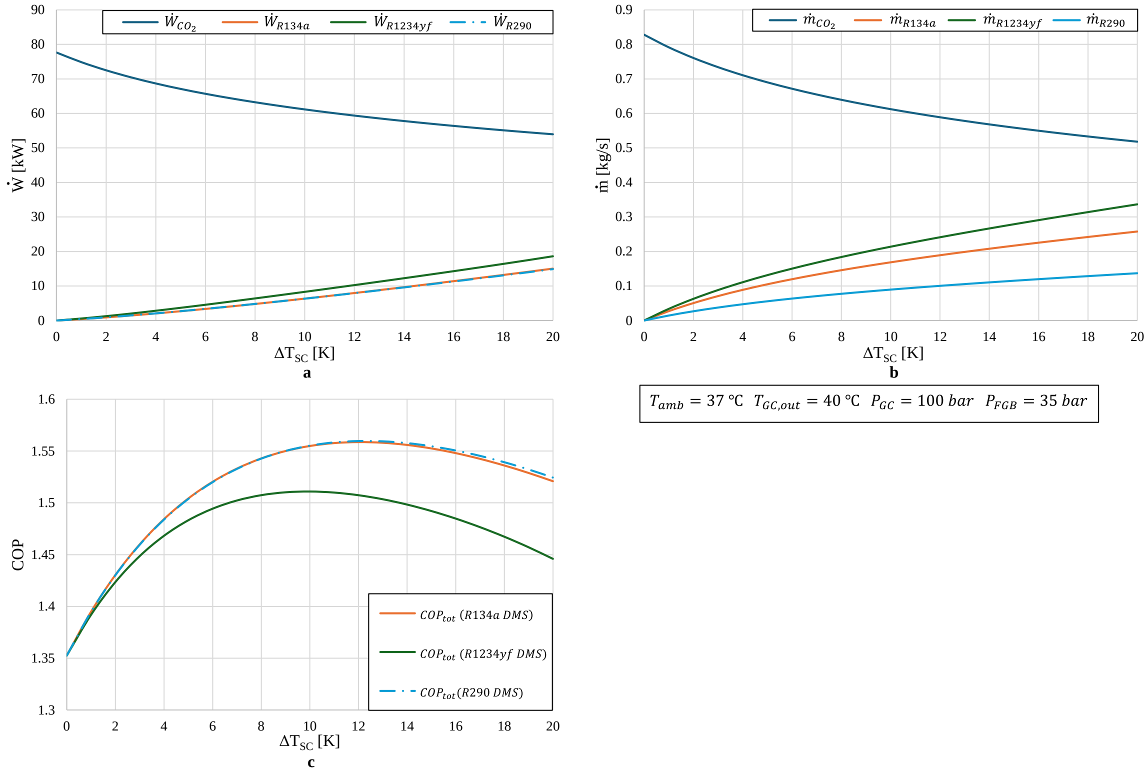


**Figure 5.** Effect of the Subcooling Degree to **a.** Power Consumptions, **b.** Mass Flow Rates, **c.** COP of BRC

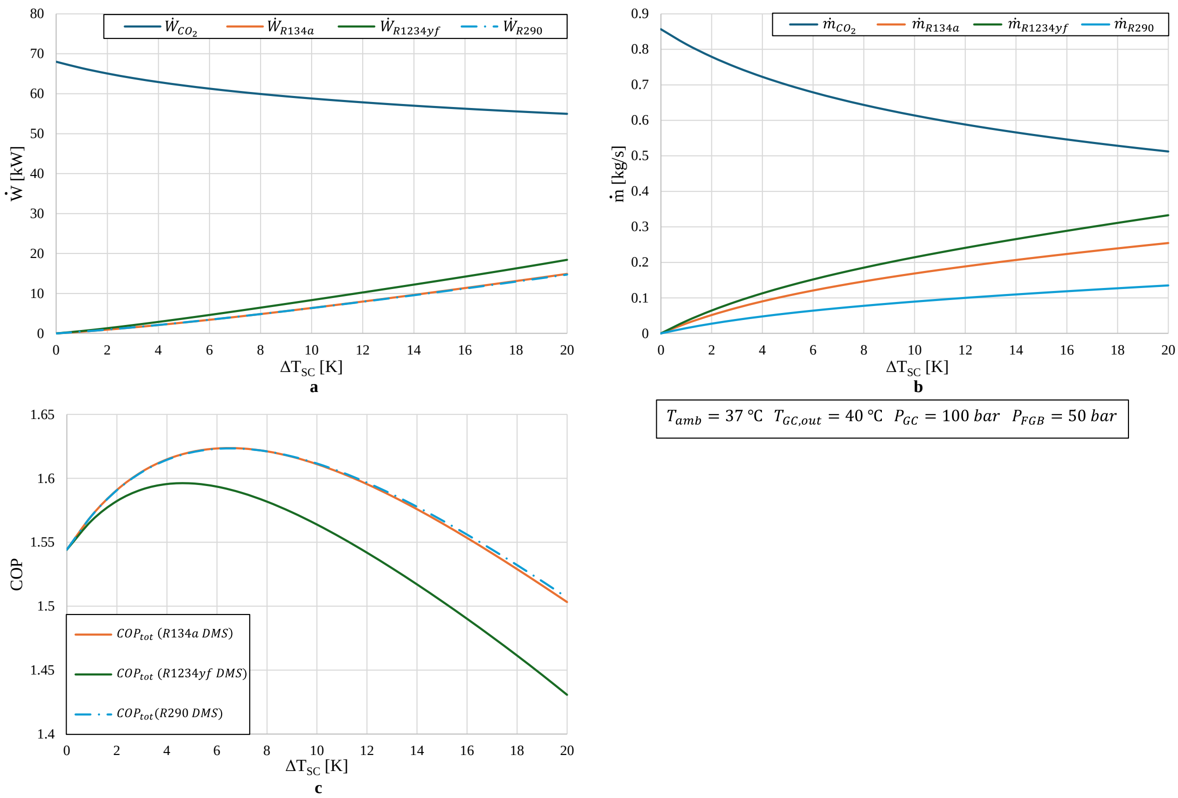


**Figure 6.** Effect of the Subcooling Degree to **a.** Power Consumptions, **b.** Mass Flow Rates, **c.** COP of PRC

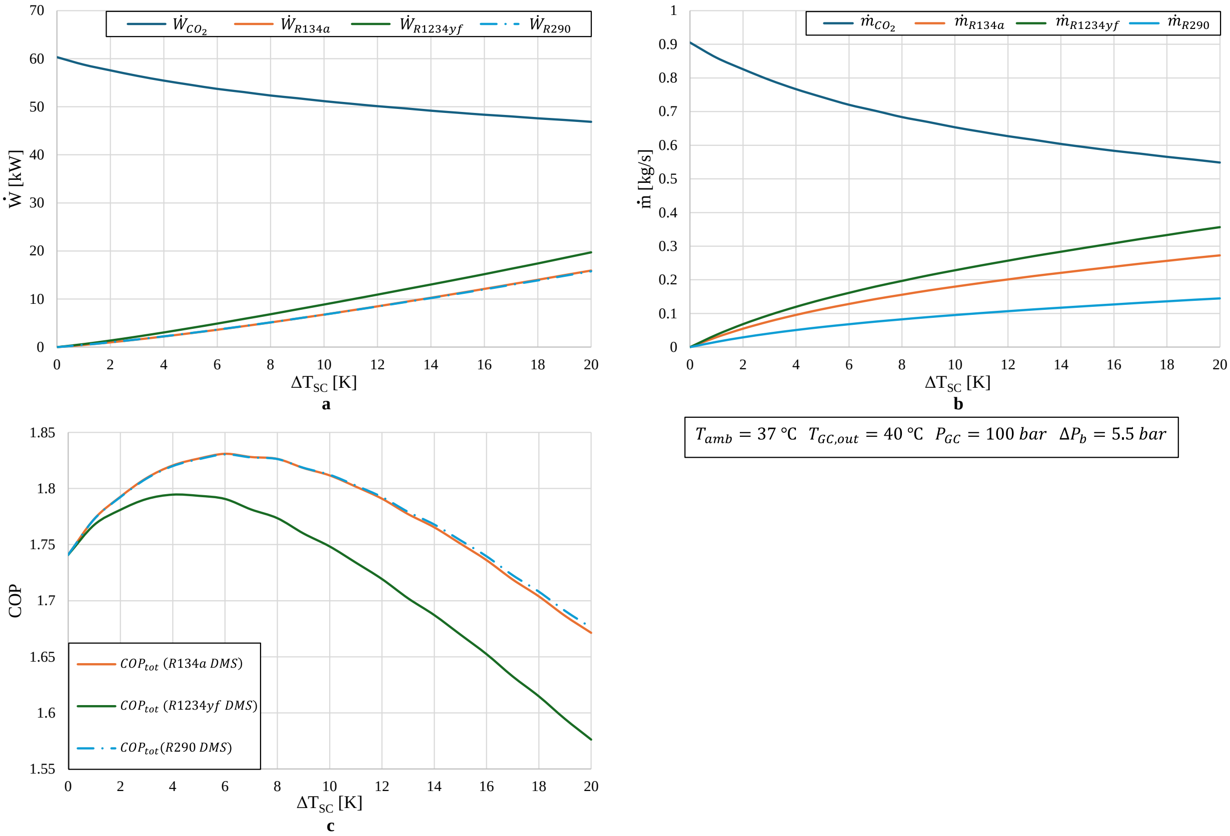


**Figure 7.** Effect of the Subcooling Degree to **a.** Power Consumptions, **b.** Mass Flow Rates, **c.** COP of ERC

Above the critical point, pressure and temperature are independent of each other. Therefore, the gas cooler pressure ($P_{GC}$) needs to be optimized under transcritical operation for all cycles. The intermediate pressure ($P_{FGB}$) in BRC was taken as 35 bar for proper feeding of the evaporators (Mitsopoulos et al., 2019). In PRC, $P_{FGB}$ is needed to be optimized as well for the maximum performance. In ERC, however, there is an optimum pressure drop in the suction nozzle ($\Delta P_b$) for maximum performance (Caliskan and Ersoy, 2022). Golden Section Search (GSS) method was used for one-variable optimization and Genetic Algorithm (GA) method was used for multi-variable optimization with the objective of minimization of the total power consumption (The MathWorks Inc., 2022). Optimized parameters for each $CO_2$ cycle are presented in Table 7.

**Table 7.** Optimized Parameters for the Investigated $CO_2$ Cycles

| Cycle | Optimized Parameters | |
|---|---|---|
| | **without DMS** | **with DMS** |
| BRC | $P_{GC}$ | $P_{GC}, \Delta T_{SC}$ |
| PRC | $P_{GC}, P_{FGB}$ | $P_{GC}, P_{FGB}, \Delta T_{SC}$ |
| ERC | $P_{GC}, \Delta P_b$ | $P_{GC}, \Delta P_b, \Delta T_{SC}$ |

The optimization process was conducted within the gas cooler outlet temperature ($T_{GC,out}$) range of 30.5 to 45 °C with 0.5 °C increments. The optimized variables of the cycles are presented in Figure 8 for BRC, Figure 9 for PRC, and Figure 10 for ERC. It is noteworthy that the optimum gas cooler pressure ($P_{GC,opt}$) is lower for all cycles with DMS compared to the ones without DMS. The difference is much higher for BRC. Decrease in $P_{GC,opt}$ is between 2.5 and 8.9 bar for BRC, between 0.5 and 6.2 bar for PRC, and between 0.1 and 6.5 bar for ERC. The optimum intermediate pressure ($P_{FGB,opt}$) does not deviate much with the increase in $T_{GC,out}$ and it is around 50 bar for PRC without DMS whereas it decreases to around 44 bar with DMS. $\Delta P_{b,opt}$ for ERC with DMS decreases from around 5.7 bar to 5.1 bar compared to the cycle without DMS. The optimum subcooling degree ($\Delta T_{SC,opt}$) is lower for R1234yf compared to R134a and R290 because of its lower performance than other refrigerants. It is seen that cycles with R134a and R290 DMS circuits have the highest performance compared to cycles without DMS and R1234yf DMS. The difference is higher at higher gas cooler outlet temperatures, and it is more significant for BRC.

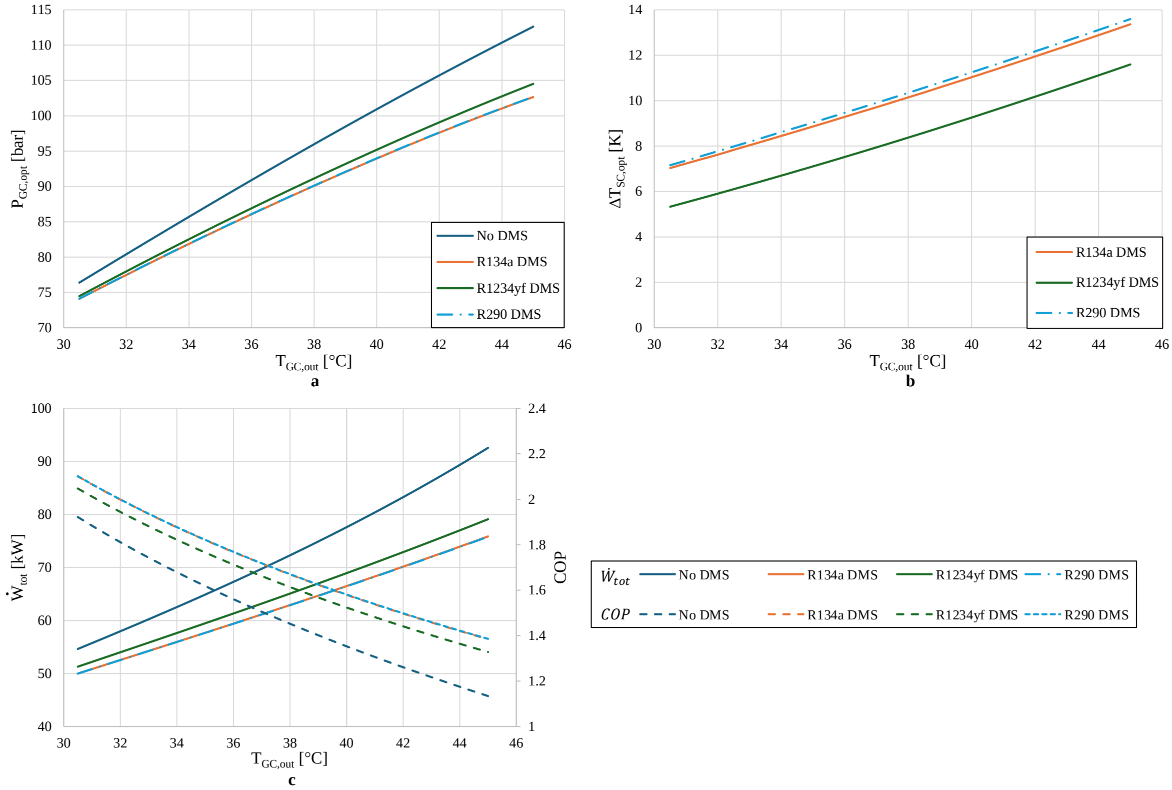


**Figure 8. a.** Optimized Gas Cooler Pressure, **b.** Optimized Subcooling Degree, **c.** Power Consumption and COP Values of BRC under Different Gas Cooler Outlet Temperatures

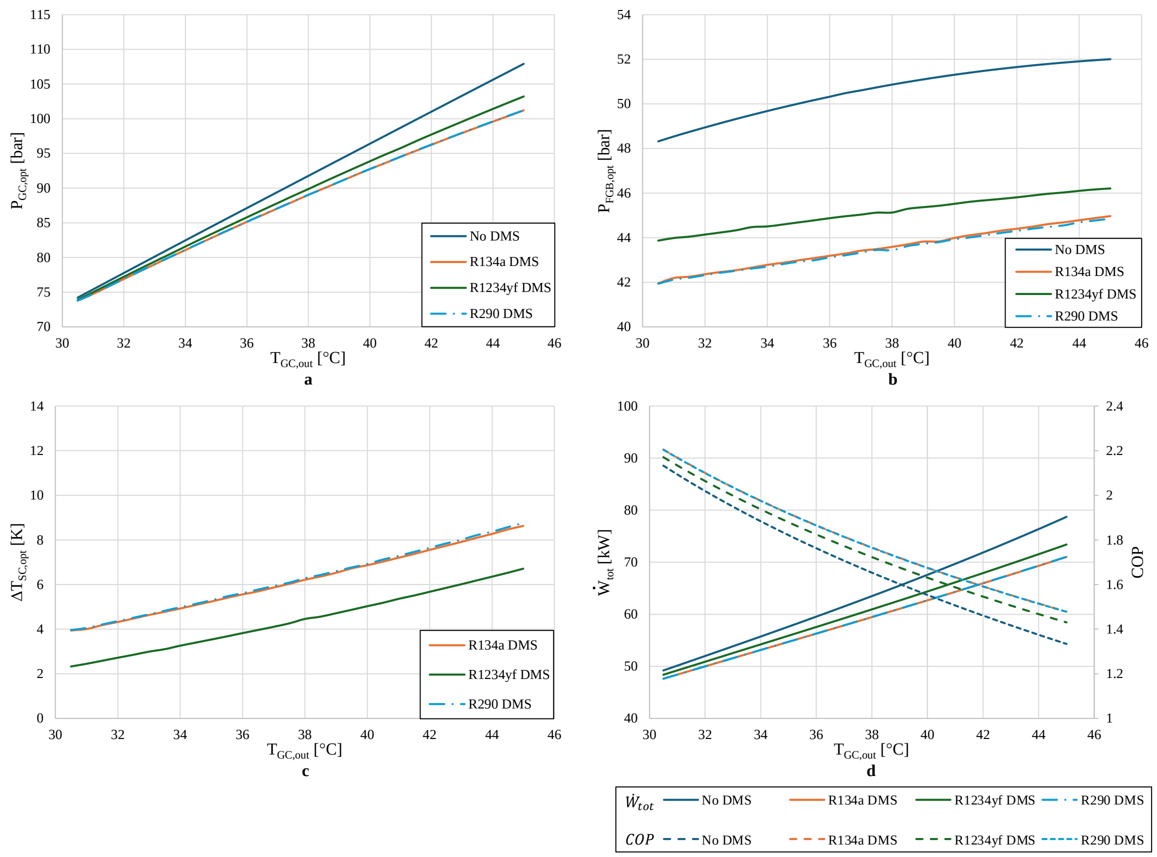


**Figure 9. a.** Optimized Gas Cooler Pressure, **b.** Optimized Intermediate Pressure, **c.** Optimized Subcooling Degree, **d.** Power Consumption and COP Values of PRC under Different Gas Cooler Outlet Temperatures

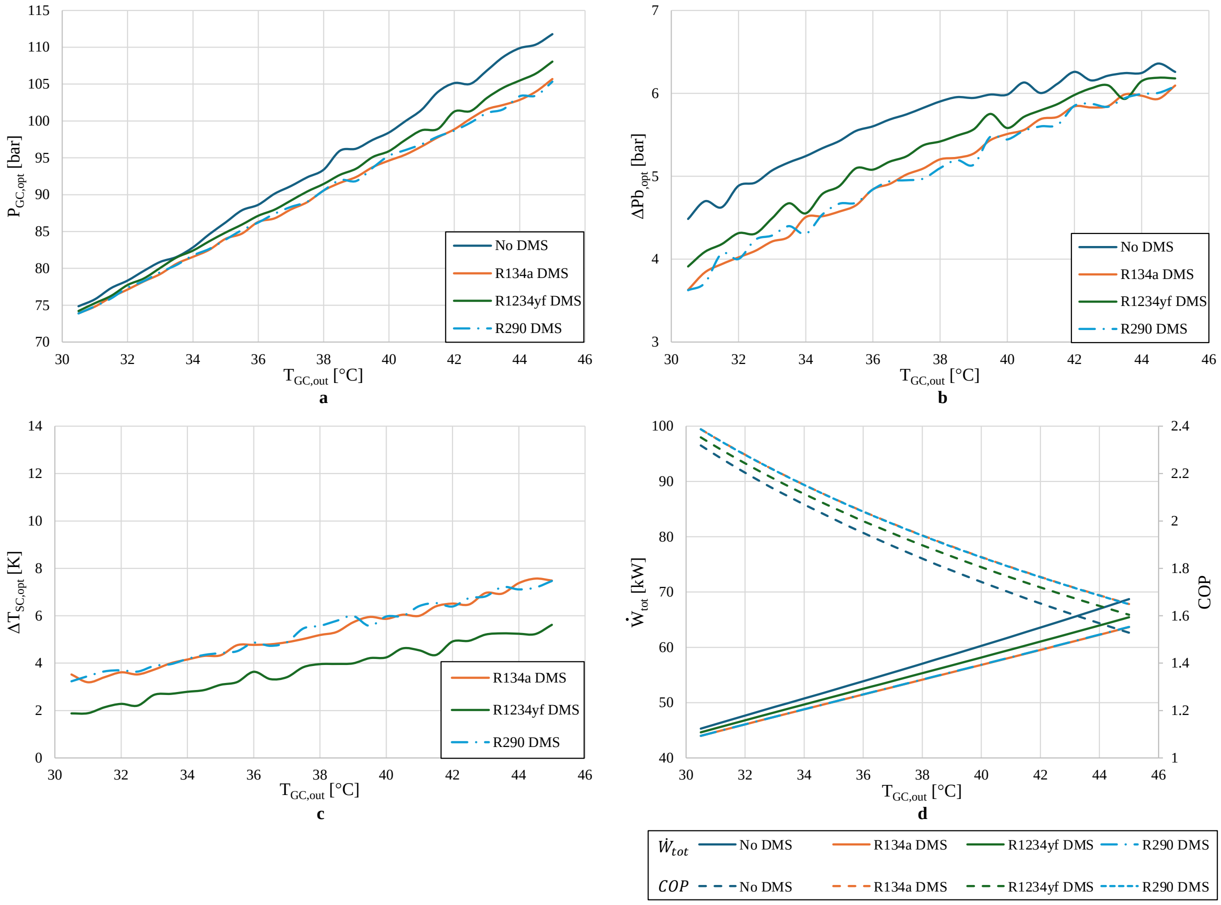


**Figure 10. a.** Optimized Gas Cooler Pressure, **b.** Optimized Suction Nozzle Pressure Drop, **c.** Optimized Subcooling Degree, **d.** Power Consumption and COP Values of ERC under Different Gas Cooler Outlet Temperatures

Entrainment ratio ($\omega$) and pressure lift ratio (ratio of the diffuser outlet pressure to the chiller pressure) values were investigated within the gas cooler outlet temperature $\left(T_{GC,out}\right)$ range of 30.5 to 45 °C using optimized values of gas cooler pressure ($P_{GC}$), suction nozzle pressure drop ($\Delta P_b$), and subcooling degree ($\Delta T_{SC}$). Entrainment ratio varies between 0.423 and 0.35 for ERC without DMS, between 0.485 and 0.434 for R134a DMS, between 0.461 and 0.417 for R1234yf DMS, and between 0.481 and 0.433 for R290 DMS. Pressure lift ratio varies between 1.31 and 1.57 for ERC without DMS, between 1.24 and 1.42 for R134a DMS, between 1.27 and 1.45 for R1234yf DMS, and between 1.25 and 1.42 for R290 DMS. As an example of the results obtained, at $T_{GC,out} = 40$ °C and $P_{GC} = 96\ bar$, entrainment ratio is 0.356 and pressure lift ratio is 1.49 for ERC without DMS, while entrainment ratio is 0.44 and pressure lift ratio is 1.37 for R290 DMS at $\Delta T_{SC} = 5$ °C. When DMS is applied to ERC, entrainment ratio increases and pressure lift ratio decreases. Since an increase in entrainment ratio has a positive effect on COP and a decrease in pressure lift ratio has a negative effect on COP, the application of DMS to ERC increases COP less than BRC.

Correlations for the optimum gas cooler pressures were derived using curve-fitting. As other parameters do not deviate much, mean values were used. Correlations for optimized variables of the investigated cycles under transcritical operation are shown in Table 8. The mean deviation of COP from the optimum values presented in Figures 8-10 is below 0.65% for each cycle.

Figure 11 presents total power consumption and COP values of each cycle depending on the ambient temperature using the correlations given in Table 8. DMS circuits operate if $T_{amb} > 27$ °C for all cycles and PC operates if $T_{amb} > 14$ °C for PRC. Subcooling is applied in the condenser under subcritical operation. Under subcritical operation, $P_{FGB}$ was taken as 40 bar for PRC and $\Delta P_b$ was taken as 3 bar for ERC. Considering the cycles without DMS, BRC has better performance than R404A system at ambient temperatures below 18 °C while PRC and ERC perform better at any ambient temperature. The performance difference of the cycles with DMS increases with the increase in the ambient temperature. It is more significant for BRC than other cycles. COP improvement of DMS is up to 20.5% for BRC, up to 9.5% for PRC, and up to 7.1% for ERC. COP improvement of BRC, PRC, and ERC with DMS compared to R404A system is up to 15.2%, 22.9%, and 37.7%, respectively. ERC cycles have the best performance among investigated cycles due to the pressure recovery in the ejector.

**Table 8.** Correlations for Optimized Variables of the Investigated Cycles under Transcritical Operation

| Cycle | $P_{GC,opt}$ [bar] | $P_{FGB,opt}$ [bar] | $\Delta P_{b,opt}$ [bar] | $\Delta T_{SC,opt}$ [K] | COP Mean Deviation |
|---|---|---|---|---|---|
| BRC without DMS | $2.505T_{GC,out} + 0.4847$ | 35 | - | - | 0.004% |
| BRC+R134a DMS<br>BRC+R1234yf DMS<br>BRC+R290 DMS | $-0.02257T_{GC,out}^2 + 3.7423T_{GC,out} - 18.02$ | 35 | - | 9.5 | 0.434%<br>0.360%<br>0.451% |
| PRC without DMS | $2.323T_{GC,out} + 3.453$ | 50 | - | - | 0.035% |
| PRC+R134a DMS<br>PRC+R1234yf DMS<br>PRC+R290 DMS | $-0.01902T_{GC,out}^2 + 3.37967T_{GC,out} - 11.63$ | 44 | - | 5.5 | 0.358%<br>0.488%<br>0.363% |
| ERC without DMS | $2.598T_{GC,out} - 4.847$ | - | 5.5 | - | 0.122% |
| ERC+R134a DMS<br>ERC+R1234yf DMS<br>ERC+R290 DMS | $-0.00457T_{GC,out}^2 + 2.5567T_{GC,out} + 0.21767$ | - | 5 | 5 | 0.339%<br>0.645%<br>0.336% |

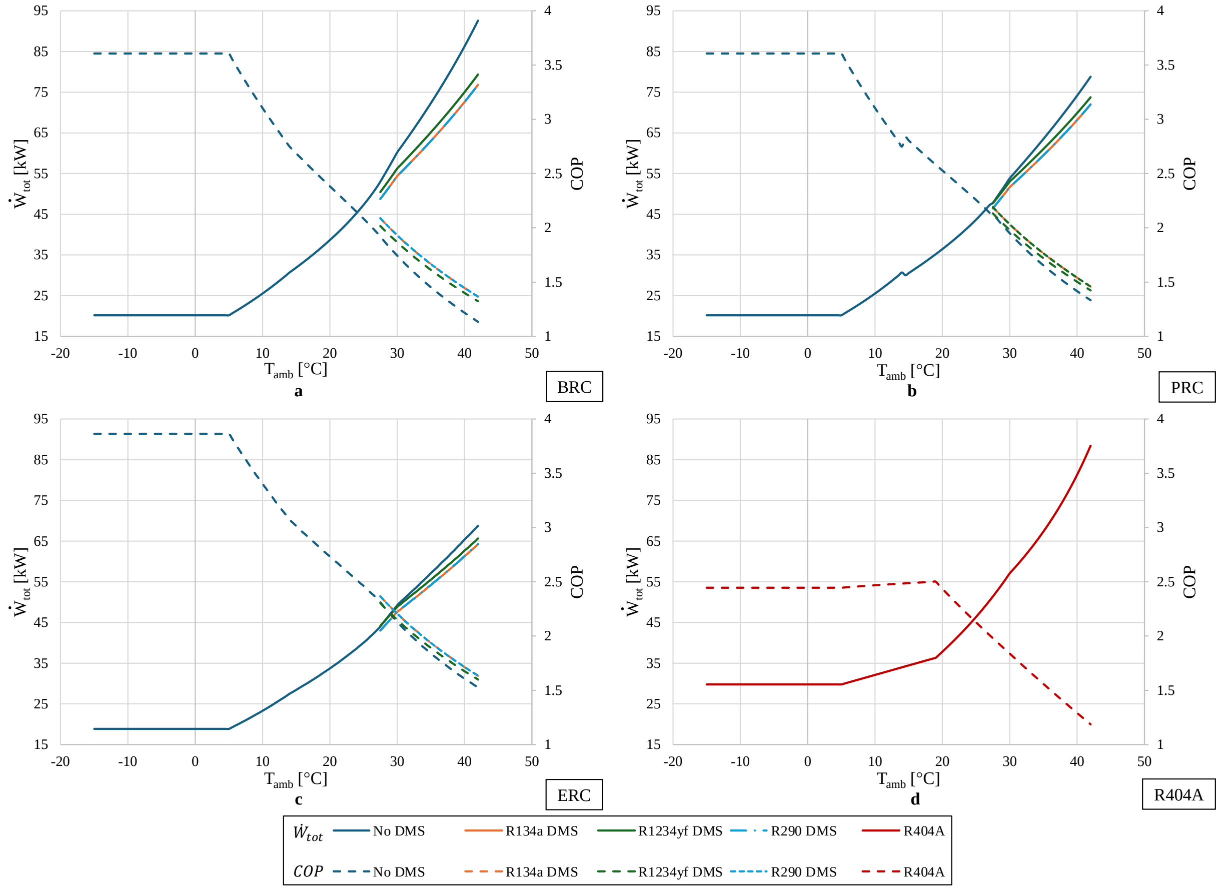


**Figure 11.** Total Power Consumption and COP Values of **a.** BRC, **b.** PRC, **c.** ERC, **d.** R404A under Different Ambient Temperatures

***Case Study for Annual Energy Consumption and Environmental Impact***

Türkiye has 5 different climate zones according to Köppen-Trewartha climate classification (Bölük and Kömüşcü, 2018). İstanbul (Cs - *subtropical dry summer*), Konya (Dc - *temperate continental*), and Samsun (Cf - *subtropical humid*) were chosen as different climate zones for annual energy consumption and TEWI comparison of the investigated cycles. Figure 12 shows the temperature bins and occurrence hours derived from meteorological data for three investigated provinces (Çalışkan and Ersoy, 2024). Transcritical operation hours are 753 for İstanbul, 788 for Konya, and 313 for Samsun considering the operation conditions shown in Table 2.

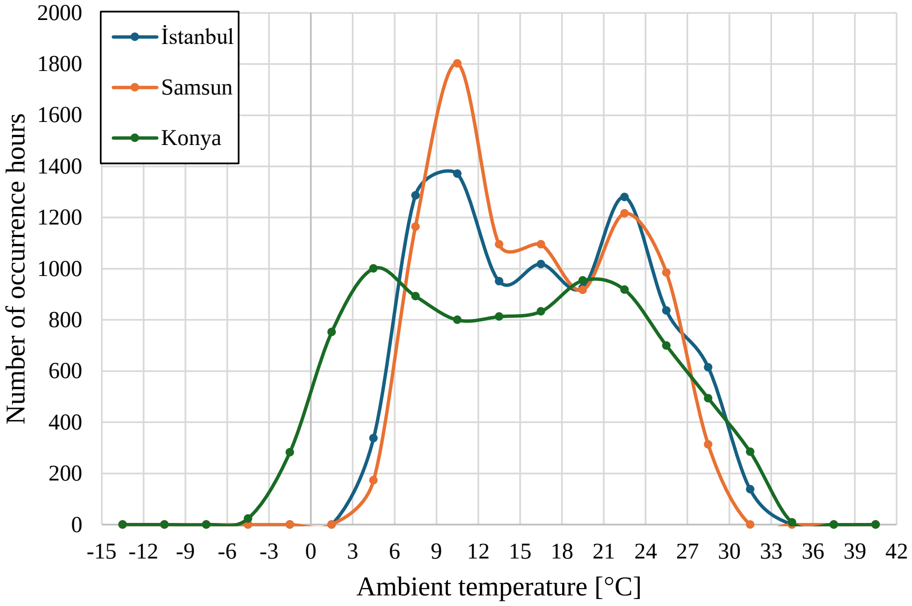


**Figure 12.** Bin-Hour Data for Three Provinces in Türkiye

Annual energy consumptions of the investigated cycles based on the bin-hour data are presented in Figure 13. R404A system has the highest energy consumption while ERC has the lowest among all cycles. As DMS operates under transcritical conditions, consumptions of the cycles with DMS are similar to the ones without DMS for Samsun, which has lower transcritical operation hours than other investigated provinces. BRC cycles with DMS have up to 8.1%, 11.1%, and 8.1% lower energy consumption compared to R404A for İstanbul, Konya, and Samsun, respectively. Energy savings of PRC cycles are up to 5.3% compared to BRC cycles without DMS whereas energy savings of ERC cycles are up to 13% and 8.6% compared to BRC and PRC cycles without DMS, respectively. Cycles with DMS have lower consumption up to 1.5% for BRC, 0.6% for PRC, and 0.5% for ERC without DMS. It can be seen that the effect of DMS is not remarkable for PRC and PRC.

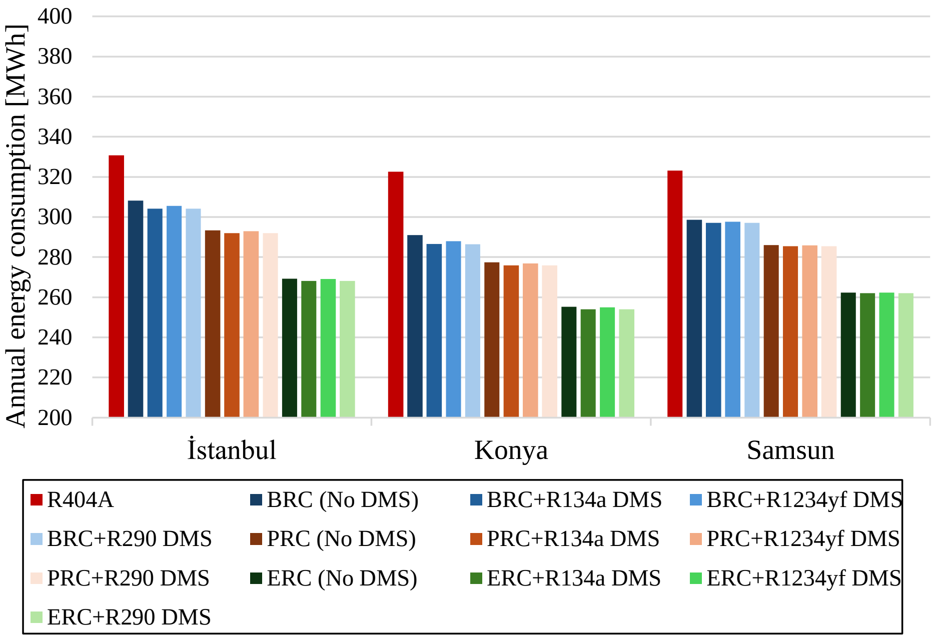


**Figure 13.** Annual Energy Consumptions of the Cycles for Investigated Provinces

Figure 14 shows the direct and total TEWI values of the investigated cycles for three provinces. R404A system has the highest direct TEWI among all investigated cycles due to its high GWP whereas $CO_2$ cycles without DMS, with R1234yf and R290 DMS have direct TEWI values below 1 ton. Cycles with R134a DMS have higher direct TEWI (up to 131.6 tons) compared to other $CO_2$ cycles because of their relatively higher GWP than $CO_2$, R1234yf, and R290. Total TEWI of R404A system is above 4000 tons while $CO_2$ cycles have total TEWI values below 2150 tons. $CO_2$ cycles with R1234yf and R290 DMS have lower total TEWI than other cycles due to their lower GWP values.

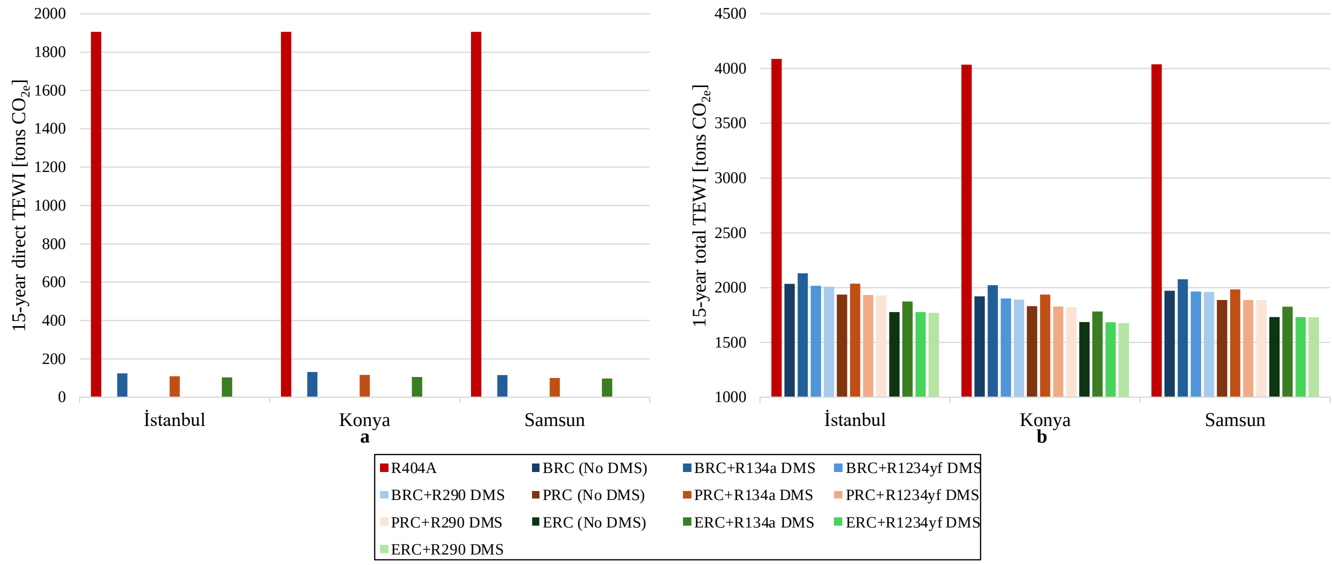


**Figure 14.** 15-Year **a.** Direct, **b.** Total TEWI Values of the Cycles for Investigated Provinces

## CONCLUSIONS

In this paper, booster (BRC), parallel compression (PRC), and ejector expansion (ERC) transcritical supermarket refrigeration cycles with dedicated mechanical subcooler (DMS) were modeled in MATLAB environment, optimum parameters were calculated using the Genetic Algorithm (GA) method for different gas cooler outlet temperatures, and correlations for the optimum parameters were derived. Performance comparison of the cycles among each other, cycles without DMS circuits, and R404A conventional system was also made. As a case study, annual energy consumption and total equivalent warming impact (TEWI) calculations were made for three different provinces in Türkiye, which are in different climate zones. The main conclusions are as follows:

- There is an optimum point for the subcooling degree to obtain the maximum COP.
- Cycles with DMS have lower optimum gas cooler pressure compared to the cycles without DMS.
- The performance difference of the cycles with DMS is more remarkable at higher ambient temperatures.
- The effect of DMS is more remarkable for BRC compared to PRC and ERC.
- ERC has the highest performance among the investigated cycles due to its pressure recovery potential.
- R404A conventional system has the highest annual energy consumption and TEWI while ERC has the lowest in the investigated provinces.
- Direct TEWI values of the $CO_2$ cycles without DMS, with R1234yf and R290 DMS are below 1 ton.
- Total TEWI values of the ejector cycles are below 2000 tons in the investigated provinces. Up to 58.4% reduction in total TEWI was obtained compared to R404A system.
- As R134a and R290 DMS cycles have identical performance, R290 could be preferred due to its lower GWP value.

## NOMENCLATURE

*Abbreviations*

AR : Assessment Report
BRC : Booster refrigeration cycle
ERC : Ejector expansion refrigeration cycle
DMS : Dedicated mechanical subcooler

FGB : Flash-gas-bypass
GA : Genetic Algorithm
GSS : Golden Section Search
HFC : Hydrofluorocarbon
HPC : High-pressure compressor
HPXV : High-pressure expansion valve
IPCC : Intergovernmental Panel on Climate Change
LPC : Low-pressure compressor
LPXV : Low-pressure expansion valve
MPXV : Medium-pressure expansion valve
PC : Parallel compressor
PRC : Parallel compression refrigeration cycle

*Symbols*
$a$ : Flow cross-sectional area [$m^2$]
$COP$ : Coefficient of performance
$E$ : Annual energy consumption [kWh]
$GWP$ : 100-year global warming potential [kg $CO_{2e}$]
$h$ : Specific enthalpy [kJ/kg]
$K$ : Electricity generation emissions [kg $CO_{2e}$/kWh]
$L$ : Annual refrigerant leakage [kg]
$m$ : Refrigerant charge [kg]
$\dot{m}$ : Mass flow rate [kg/s]
$mf$ : Minimum fraction
$N$ : Number of temperature bin occurrence hours
$n$ : Operation lifetime [years]
$T$ : Temperature [°C]
$TEWI$ : Total equivalent warming impact [kg $CO_{2e}$]
$P$ : Pressure [bar]
$\dot{Q}$ : Heat transfer rate [kW]
$R_p$ : Pressure ratio
$s$ : Specific entropy [kJ/kg K]
$u$ : Velocity [m/s]
$v$ : Specific volume [$m^3$/kg]
$\dot{W}$ : Power consumption [kW]

*Greek Letters*
$\alpha$ : Refrigerant recycling factor
$\varepsilon$ : Heat exchanger effectiveness
$\eta$ : Efficiency
$\omega$ : Ejector entrainment ratio

*Subscripts*
amb : Ambient
b : Ejector suction nozzle outlet
comp : Compressor
cond : Condenser
dif : Diffuser
ev : Evaporator
GC : Gas cooler
glob : Global
is : Isentropic
LT : Low-temperature (freezer)
m : Ejector mixing chamber outlet
mn : Motive nozzle

MT : Medium-temperature (chiller)
opt : Optimum
ref : Refrigerant
SC : Subcooling
sn : Suction nozzle
tot : Total

**REFERENCES**

Atmaca, A. U., Erek, A., Ekren, O., & Çoban, M. T. (2018). Thermodynamic performance of the transcritical refrigeration cycle with ejector expansion for R744, R170, and R41. *Journal of Thermal Science and Technology, 38*, 111–127.

Bell, I. H., Wronski, J., Quoilin, S., & Lemort, V. (2014). Pure and Pseudo-pure Fluid Thermophysical Property Evaluation and the Open-Source Thermophysical Property Library CoolProp. *Industrial & Engineering Chemistry Research, 53*(6), 2498–2508. https://doi.org/10.1021/ie4033999

Bölük, E., & Kömüşcü, A. Ü. (2018). *Köppen-Trewartha iklim sınıflandırmasına göre Türkiye iklimi*. Ankara, Türkiye: Directorate General of Meteorology.

Caliskan, O., Bilir Sag, N., & Ersoy, H. K. (2024). Thermodynamic, environmental, and exergoeconomic analysis of multi-ejector expansion transcritical CO2 supermarket refrigeration cycles in different climate regions of Türkiye. *International Journal of Refrigeration*, *165*, 466–484. https://doi.org/10.1016/j.ijrefrig.2024.05.006

Caliskan, O., & Ersoy, H. K. (2022). Energy analysis and performance comparison of transcritical CO2 supermarket refrigeration cycles. *The Journal of Supercritical Fluids*, *189*, 105698. https://doi.org/10.1016/j.supflu.2022.105698

Çalışkan, O., & Ersoy, H. K. (2024). Energy, environmental, and exergoeconomic (3E) analysis of transcritical CO2 booster and parallel compression supermarket refrigeration cycles in climate zones of Türkiye. *Konya Journal of Engineering Sciences*, 123–137. https://doi.org/10.36306/konjes.1393426

Catalán-Gil, J., Llopis, R., Sánchez, D., Nebot-Andrés, L., & Cabello, R. (2019). Energy analysis of dedicated and integrated mechanical subcooled CO2 boosters for supermarket applications. *International Journal of Refrigeration*, *101*, 11–23. https://doi.org/10.1016/j.ijrefrig.2019.01.034

Chakroun, W. (2016). *Lower-GWP Alternatives in Commercial and Transport Refrigeration: An expanded compilation of propane, CO2, ammonia and HFO case studies*. Paris: United Nations Environment Programme.

Contiero, L., Pardiñas, A. A., & Hafner, A. (2021, September 16). *Multi ejector and pivoting-supported R744 application with AC for supermarkets.* Presented at the 9th IIR Conference on Ammonia and CO2 Refrigeration Technologies, Ohrid, North Macedonia. Ohrid, North Macedonia. http://dx.doi.org/10.18462/iir.nh3-co2.2021.0019

Dai, B., Cao, Y., Zhou, X., Liu, S., Fu, R., Li, C., & Wang, D. (2024). Exergy, carbon footprint and cost lifecycle evaluation of cascade mechanical subcooling CO2 commercial refrigeration system in China. *Journal of Cleaner Production*, *434*, 140186. https://doi.org/10.1016/j.jclepro.2023.140186

Danfoss. (2023). *Coolselector2*. Danfoss A/S.

de Paula, C. H., Duarte, W. M., Rocha, T. T. M., de Oliveira, R. N., & Maia, A. A. T. (2020). Optimal design and environmental, energy and exergy analysis of a vapor compression refrigeration system using R290, R1234yf, and R744 as alternatives to replace R134a. *International Journal of Refrigeration*, *113*, 10–20. https://doi.org/10.1016/j.ijrefrig.2020.01.012

de Paula, C. H., Duarte, W. M., Rocha, T. T. M., de Oliveira, R. N., Mendes, R. de P., & Maia, A. A. T. (2020). Thermo-economic and environmental analysis of a small capacity vapor compression refrigeration system using R290, R1234yf, and R600a. *International Journal of Refrigeration*, *118*, 250–260. https://doi.org/10.1016/j.ijrefrig.2020.07.003

Devotta, S., & Sicars, S. (2005). Refrigeration. In *IPCC/TEAP Special Report: Safeguarding the Ozone Layer and the Global Climate System*. Cambridge University Press. Retrieved from https://archive.ipcc.ch/pdf/special-reports/sroc/sroc04.pdf

ETKB. (2022). *Türkiye elektrik üretimi ve elektrik tüketim noktası emisyon faktörleri bilgi formu* (No. ETKB-EVÇED-FRM-042 Rev.00). Ankara, Türkiye: Ministry of Energy and Natural Resources.

Haroldsen, J. O. (2023, June 21). Japanese C-Store Operator Lawson Operates 5,028 Stores – Over 34% of Its Chain – With CO2 Refrigeration. Retrieved August 22, 2023, from R744.com website: https://r744.com/japanese-c-store-operator-lawson-operates-5028-stores-over-34-of-its-chain-with-co2-refrigeration/

Hayes, C. (2023, February 20). METRO Continues Rollout of Transcritical CO2 in All New Stores. Retrieved March 27, 2024, from R744 website: https://r744.com/atmo-europe-metro-continues-rollout-of-transcritical-co2-in-all-new-stores-and-refurbishments/

Hayes, C. (2024, January 15). METRO Rolls Out First Transcritical CO2 Installation in Serbia. Retrieved March 26, 2024, from R744 website: https://r744.com/metro-rolls-out-first-transcritical-co2-installation-in-serbia/

Hayes, C., Haroldsen, J., & Thapa, S. (2023). *Natural Refrigerants: State of the Industry/Refrigeration in Europe, North America and Japan, Plus Heat Pumps in Europe*. ATMOsphere.

Hines, M. (2024, January 11). All ALDI US Stores Will Transition to Natural Refrigerants by 2035. Retrieved March 26, 2024, from R744 website: https://r744.com/all-aldi-us-stores-will-transition-to-natural-refrigerants-by-2035/

Isik, M., & Bilir Sag, N. (2023). Energetic, economic, and environmental analysis of CO2 booster refrigeration systems of supermarket application for Türkiye. *Sādhanā*, *48*(4), 275. https://doi.org/10.1007/s12046-023-02337-3

Karampour, M., & Sawalha, S. (2018). State-of-the-art integrated CO2 refrigeration system for supermarkets: A comparative analysis. *International Journal of Refrigeration*, *86*, 239–257. https://doi.org/10.1016/j.ijrefrig.2017.11.006

Keenan, J. H., Neumann, E. P., & Lustwerk, F. (1950). An Investigation of Ejector Design by Analysis and Experiment. *Journal of Applied Mechanics*, *17*(3), 299–309. https://doi.org/10.1115/1.4010131

Klein, S. A. (2020). *Engineering Equation Solver*. F-Chart Software.

Klemick, H., Kopits, E., & Wolverton, A. (2015). *The Energy Efficiency Paradox: A Case Study of Supermarket Refrigeration System Investment Decisions* (No. Working Paper # 15-03). Washington DC, US: U.S. Environmental Protection Agency.

Li, D., & Groll, E. A. (2005). Transcritical CO2 refrigeration cycle with ejector-expansion device. *International Journal of Refrigeration*, *28*(5), 766–773. https://doi.org/10.1016/j.ijrefrig.2004.10.008

Liu, X., Yu, K., Wan, X., & Li, X. (2021). Performance evaluation of CO2 supermarket refrigeration system with multi-ejector and dedicated mechanical subcooling. *Energy Reports*, *7*, 5214–5227. https://doi.org/10.1016/j.egyr.2021.08.110

Mitsopoulos, G., Syngounas, E., Tsimpoukis, D., Bellos, E., Tzivanidis, C., & Anagnostatos, S. (2019). Annual performance of a supermarket refrigeration system using different configurations with CO2 refrigerant. *Energy Conversion and Management: X*, *1*, 100006. https://doi.org/10.1016/j.ecmx.2019.100006

Papazahariou, C. (2010). *Natural refrigerants faster to market, commercial refrigeration with low gwp alternatives*. Presented at the Joint Meeting of the Regional Ozone Networks for Europe & Central Asia and South Asia, Istanbul. Istanbul: Shecco.

Said, S. A. M., Habib, M. A., & Iqbal, M. O. (2003). Database for building energy prediction in Saudi Arabia. *Energy Conversion and Management*, *44*(1), 191–201. https://doi.org/10.1016/S0196-8904(02)00042-0

Schulz, M., & Kourkoulas, D. (2014). *Regulation (EU) No 517/2014 of the European Parliament and of the Council of 16 April 2014 on fluorinated greenhouse gases and repealing Regulation (EC) No 842/2006* (No. 517/2014; p. L150/195-230). Retrieved from http://eur-lex.europa.eu/eli/reg/2014/517/oj

Sengupta, A., & Dasgupta, M. S. (2023). Energy and advanced exergoeconomic analysis of a novel ejector-based CO2 refrigeration system and its optimization for supermarket application in warm climates. *Thermal Science and Engineering Progress*, *44*, 102056. https://doi.org/10.1016/j.tsep.2023.102056

Smith, C., Nicholls, Z. R. J., Armour, K., Collins, W., Forster, P., Meinshausen, M., … Watanabe, M. (2021). The Earth's Energy Budget, Climate Feedbacks, and Climate Sensitivity Supplementary Material (V. Masson-Delmotte,

P. Zhai, A. Pirani, S. L. Connors, C. Péan, S. Berger, … B. Zhou, Eds.). Retrieved from https://www.ipcc.ch/report/ar6/wg1/downloads/report/IPCC_AR6_WGI_Chapter07_SM.pdf

The MathWorks Inc. (2022). *MATLAB version: 9.13.0.2399474 (R2022b) update 7*. The MathWorks Inc. Retrieved from www.mathworks.com

Tsamos, K. M., Ge, Y. T., Santosa, Id., Tassou, S. A., Bianchi, G., & Mylona, Z. (2017). Energy analysis of alternative CO 2 refrigeration system configurations for retail food applications in moderate and warm climates. *Energy Conversion and Management*, *150*, 822–829. https://doi.org/10.1016/j.enconman.2017.03.020

Tsimpoukis, D., Syngounas, E., Petsanas, D., Mitsopoulos, G., Anagnostatos, S., Bellos, E., … Vrachopoulos, M. G. (2021). Energy and environmental investigation of R744 all-in-one configurations for refrigeration and heating/air conditioning needs of a supermarket. *Journal of Cleaner Production*, *279*. https://doi.org/10.1016/j.jclepro.2020.123234

Yapici, R., & Ersoy, H. K. (2005). Performance characteristics of the ejector refrigeration system based on the constant area ejector flow model. *Energy Conversion and Management*, *46*(18–19), 3117–3135. https://doi.org/10.1016/j.enconman.2005.01.010

Zhang, M. (2006). Energy Analysis of Various Supermarket Refrigeration Systems. *International Refrigeration and Air Conditioning Conference*. Purdue.

Zottl, A., Lindahl, M., Nordman, R., Rivière, P., & Miara, M. (2011). *Evaluation method for comparison of heat pump systems with conventional heating systems, D4.3. Concept for evaluation of CO2-reduction potential*. European Commission.